Section A-Research paper

Analysis of Nanoparticles and Inorganic Components in Commercial Paints through X-ray Powder Diffraction Techniques

[1]Padmini Pandey, [2]U. V. Kiran*

[1,2]Department of Human Development and Family Studies, School for Home Sciences, Babasaheb Bhimrao Ambedkar University (A Central University), Lucknow – 226025, Uttar Pradesh, India; druvkiran@gmail.com*, dolly15pandey@gmail.com

Abstract

Several commercial paints are deployed for diverse operational requirements in the painting industry. Paint provides the primary functions such as improving the surface appearance and facilitating surface safety when exposed to the physical environment such as water, air, sunlight, etc., in vast proportions worldwide. Therefore, it is essential to examine the commercial paints using different laboratory techniques before they can be optimized and generalized for various industrial and domestic purposes. Material components and the structural analysis of the paint have been performed in the present work. The elemental compositions were obtained based on the EDX and X-ray diffraction techniques. EDX techniques are found to be useful for elemental composition. In the present research, the crystalline characteristic of the paint was also examined using diffraction peak analysis through the XRD technique. Classification of paints, accomplished using these laboratory techniques, has been categorized into several types, such as synthetic, organic, inorganic, and metallic paints.

Keywords: Commercial paint; X-ray diffraction techniques; Structural Analysis; Elemental compositions; EDX

Introduction

The painting industry is one of the most demanding industries in the commercial and manufacturing industries. New paints are developing every day with some modified properties. The Indian paint industry, which generated U.S. $7.1 billion in financial year (F.Y.) 2020, is valued at approximately 0.004375% of the total global production by paint industries, generating revenue of US$160bn. Asia Pacific (APAC), the world's largest coatings market with a 45% share valued at US$71bn+ in 2019, has grown faster than the global market due to relatively higher economic growth, especially in China and India. The aesthetic coating market (market share of 79-80%) has expanded at a CAGR of 11.4 percent,

while the commercial coating market (revenue growth of 20-25%) has risen at a CAGR of 7.9% (Punmiya, 2020).

Recent data from Occupational Safety and Health (2020) report that the paint and pigment industries are responsible for health and environmental hazards (OSH, 2020). In fact, of all professions, construction and maintenance painters have one of the highest injury rates, as reported by the Bureau of Labour Statistics (Januzzi & Wolfe, 2016).

Paint industries are constantly using hazardous chemicals in the production of their final products. Now a days, many pigments, stabilizers, binders, etc., are replaced by specific nanoparticles and micro materials with the same functional characteristics, which are essential for construction purposes. Nanomaterial's have prompted considerable intrigue as a continuously emerging field of advanced materials with broad applications (Srinivas, 2018, Sadiku et al., 2018). The physical properties of nanoparticles such as size, crystal structure, elemental composition, etc. are characterised using several techniques since the human eye is most vulnerable to the light beam, it can be determined from the current statistics that the particle dimension of paints should be relatively below the wavelength of light to be scattered (wavelength of about 0.55 microns) (Padmanabhan and John, 2020).

Significance of nanoparticles is constantly increasing in basic research and applications. Two significant variables studied in the characterization of nanoparticles are size and shape (Chen et al., 2022). Size distribution, degree of aggregation, surface charge, surface area and surface chemistry can also be measured. The first step after nanoparticle synthesis is investigating the chemical composition and crystalline structure (Kim et al., 2021). Nanoparticles are the inorganic constituents of paints and are present in crystalline forms; also, they have a stronger scatter X-rays than their organic constituents, so identifying nanoparticles became easy through XRD technique (Holder & Schaak, 2019; Hiley et al., 2022). To reduce issues with paint quality, characterization of paint samples is very much required at the microscopic level to develop a scientific and quantitative specification and standardize raw materials from various sources based on these specified requirements (Loganina & Uchaeva, 2020; Thakur et al., 2021). The primary benefit of such XRD analysis is that it can determine the chemical nature of crystal structures instead of their elemental analysis. Various composable aspects of the same compound can be easily identified in a mixture of two or more phases; and, finally, pigment powders can be analyzed in their natural state without any extensive specimen preparation (Solano et al., 2020). This study used XRD and EDX techniques to identify and

characterize the component analysis, nanoparticles and inorganic materials in commercial paints.

Experimental Analysis

Sample collection and reagents

The white color of water-based, solvent-based, and distemper liquid paints were purchased from an authorized shop of the paint (Shri Pita Maruti Iron Store Pvt. Ltd., Telibagh, Lucknow, Uttar Pradesh, India). The degraded paint sample was collected from one of the building of the Babasaheb Bhimrao Ambedkar University, which is degraded due to excess water and microbial growth. Measurements were carried out on four sample groups: solvent-based paint, water-based paint, distemper, and degraded paint chip flex. All the sample colours were kept the same to minimize the effect of color differences.

Table 1: Specifications for drying the samples

S.N.	Sample name	Sample phase	Drying time and temperature	Mode of drying
1.	Water-based paint	Fresh Liquid paint (white color)	Forty days at 90°F temp.	Dehydrator
			Thirty days at 150°F temp.	Oven
2.	Solvent-based paint	Fresh liquid paint (white color)	Thirty days at 90°F temp.	Dehydrator
			30 days at 150°F temp.	Oven
3.	Distemper paint	Fresh liquid paint (white color)	4-5 hours at 90° F temp.	Dehydrator
4.	Degraded flex paint	Degraded paint flex (white color)	Two hours to remove moisture at 90°F temp.	Dehydrator

Sample preparation

All liquid paint samples are dried in the oven and prepared as a powder material. Degraded paint flex is also converted into powder form by grinding to avoid possible polymorphic phase changes. The process of preparing the sample is illustrated in Fig.1. Fig. 2 shows the prepared sample for the analysis.

The following steps were followed to prepare the samples for analysis –

- **Weighing raw paints:** This is the first step for sample preparation. In order to keep the samples dry, 100 ml of each is measured using a weighing machine and then placed in borosil beakers.
- **Drying of paints:** The liquid paint samples in equal quantities were dried in the oven and dehydrator to prepare as powder material. They were dried using a dehydrator at 90°F temperatures for the first 30 days. Afterwards, it was placed into an oven to dry rapidly for 30 days at 150°F for 6 hours a day. Degraded paint flex was dried only in the dehydrator for two hours. However, distemper liquids took only two days to dry in an oven at 150°F, as the paint's flex was just required to release moisture, which was then quickly grounded into fine powdered form.
- **Grinding of dry paints:** Dried samples were placed into the grinder to convert into powder form to avoid possible polymorphic phase changes. A mechanical grinder and mortar pistil were used for this process.
- **Sieving of ground paints:** Ground paint samples were sieved through a 325-mesh sieve (45 mm). 325 mesh sieves are used for particle sizing applications for various fine materials.
- **Collection of Powder sample:** Finely powdered forms of the sample have been collected and stored in a sample box

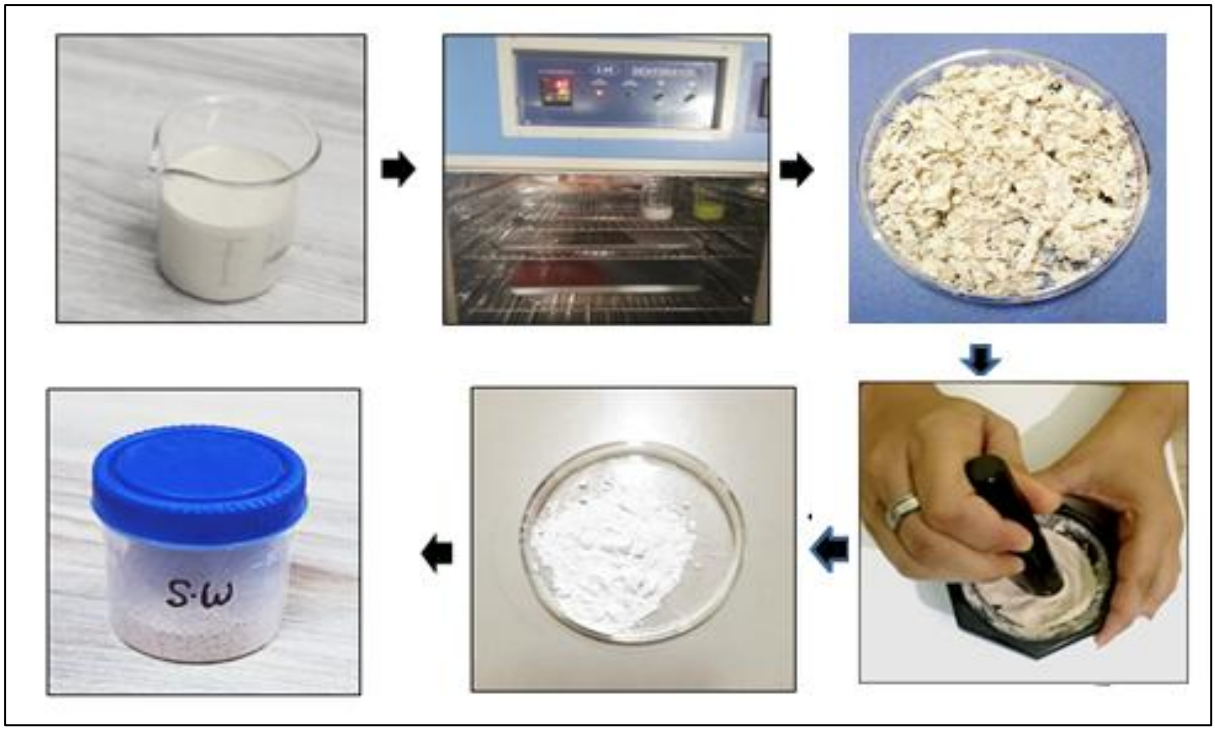

Fig. 1: Preparation of powdered sample

Fig. 2: Prepared samples 1) Water-based paint 2) Solvent-based paint 3) Distemper 4) Degraded flexes paint.

Characterization techniques

Samples were analyzed using XRD and EDX techniques.

XRD Technique (X-Ray Diffraction)

XRD has long been used to analyse pigments, including crystal structure, composition, crystalline grain size, and elemental-chemical composition (Fay et al., 2005). It is an essential and significant tool for characterizing nanoparticles in paints (Debnath & Vaidya, 2006). Crystalline compounds are identified using the current research to identify crystalline compounds in the selected samples. XRD equipment available in the USIC (University science instrumentation center) laboratory of the University was used for the experimental research. Goniometer, X-ray source, Tube housing, Mount, Sample holder, and Sensor with Lenses, Slits mechanisms and anode x-ray tube were all included in the system **(Anand et al., 2022).** DIFFRAC (EVA evaluation software), DIFFRAC (TOPAS software) for diffractogram analysis, and the ICDD PDF-4 Axiom 2020 repository are all components of this technology.

SEM/EDX

Scanning Electron Microscopy-energy dispersive X-ray analysis (SEM-EDS) can be used to characterize paint samples' morphology and elemental composition **(Manship et al., 2021).** In order to identify the composition of the sample, paint samples have been investigated by EDX techniques by the model JSM 6490 LV. Modern technical advancement broadens their scope of use and strengthens their effectiveness as potent tools for characterizing paints **(Hadimani, 2018; Guglielmi et al., 2022)**.

Analysis

The diffraction outputs of the identified samples are presented in table 2. The data is organized by composition, and the complete specimen has been used to create the diffraction pattern. Coatings are composed of various ingredients, including a binder, solvents, resin, pigments, and extenders.

Table 2: Paint compositional output through XRD

S.N.	Sample name	Elements identified
1.	Water-based paint	Rutile, syn (TiO_2), calcite, syn $Ca(CO_3)$, Cerium Hydrogen Phosphate Hydrate ($CeH(PO_3H)_2 \cdot H2O$)
2.	Solvent-based paint	Rutile, syn (TiO_2), Titanium Vanadium Oxide ($TiO_5V_2O_5$), Calcium Zinc Vanadate $Ca_2Zn_2(V_3O_{10})(VO_4)$

3.	Distemper	Dolomite, $CaMg(CO_3)_2$, Calcite magnesian, syn $(Mg0.03Ca0.97)(CO_3)$, Silicon dioxide (SiO_2)
4.	Degraded flex paint	Dolomite $CaMg(CO3)_2$, Calcite $Ca0.936Mg0.064(CO_3)$, magnesium, Barium Niobium Oxide Hydroxide $Ba_6Nb_3O13(O.H.)$

Fresh paint samples of both the water-based and solvent-base have similar nanoparticle TiO_2 that is in the rutile phase, as shown in Table 2. On the other hand, calcite and calcium compounds are found in all the samples. Dolomite is calcium and magnesium chemical commonly used in all types of paints, mainly local paints. SiO_2 (anatase) was also detected in distemper paint.

Various components included in the paint samples were identified by analysing the XRD spectra of the samples with standard diffractometer provided in Figs. 3-6. Set of paints selected for characterization are shown in fig. 3, 4, 5, and 6 along with images. For the convenience of discussion, first the nanoparticles were presented, followed by inorganic substances.

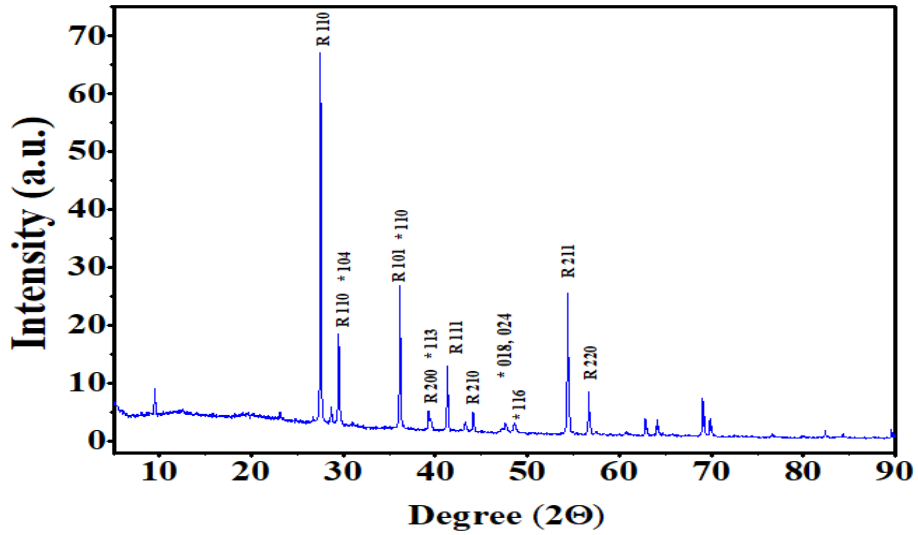

Fig. 3: XRD pattern of fresh water-based paint, where (R and *) are Miller indices of peaks attributed to Rutile TiO_2 and Calcite, respectively.

Fig. 3 presents the diffraction findings within 10–90° diffraction angle range, with the highly relevant peaks corresponding to Rutile TiO_2 nanoparticles and calcite. These peaks are located at 2θ (Miller indices) = 27.38° (1 1 0), 29.38° (1 1 0), 35.99° (1 0 1), 39.17° (2 0 0),

41.39° (1 1 1), 44.18° (2 1 0), 54.22° (2 1 1), 56.63° (2 2 0) for Rutile TiO_2 nanoparticle. Calcite peaks are located at 2θ (Miller indices) = 23° (0 1 2), 29.46° (1 0 4), 36.12° (1 1 0), 39.53° (1 1 3), 47.81° (0 1 8) (0 2 4), 48.89° (1 1 6) 57.70° (1 2 2). They are well matched with the JCPDS # 75-1537 (El-Desoky et al., 2020) and ICSD 073446 (Deng et al., 2010). TiO_2 is the main pigment used in water-born paints due to its high refractive index and coverage capability.

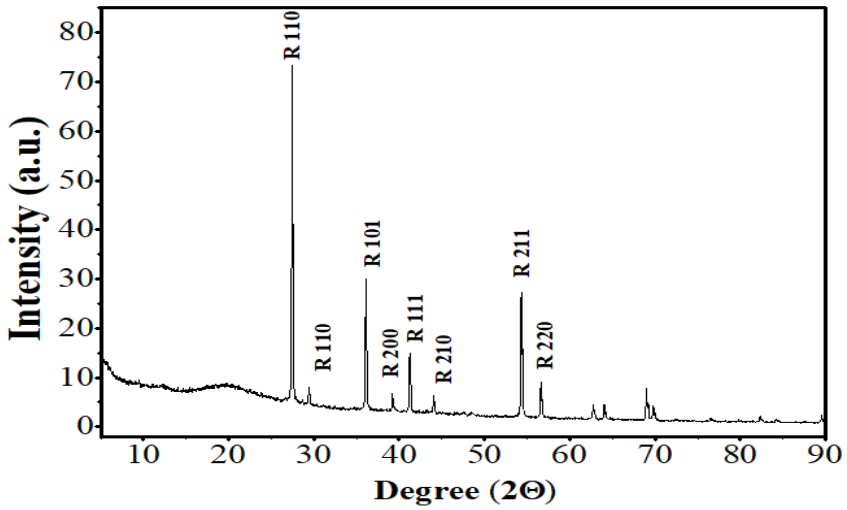

Fig. 4: XRD pattern of fresh solvent-based paint (Sample.2 S.W.), where (R) are Miller indices of peaks attributed to Rutile TiO_2.

Fig. 4 illustrates the XRD finding with the most significant peaks belonging to Rutile TiO_2 nanoparticles in an angular frequency range of 10–90°. These peaks are located at 2θ (Miller indices) = 27.38° (1 1 0), 29.38° (1 1 0), 35.99° (1 0 1), 39.17° (2 0 0), 41.39° (1 1 1), 44.18° (2 1 0), 54.22° (2 1 1) for Rutile TiO_2 nanoparticle. It seemed well matched with the JCPDS # 75-1537 (El-Desoky et al., 2020).

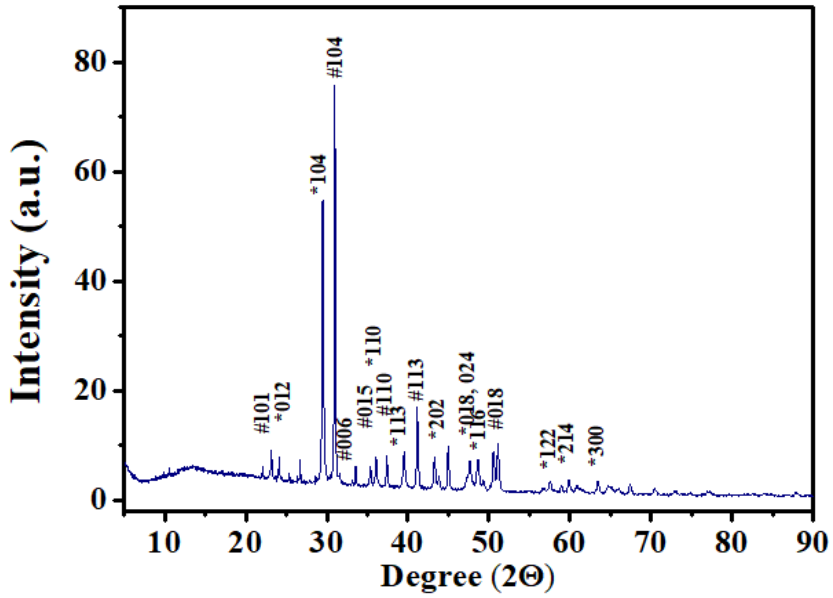

Fig. 5: XRD pattern of used distemper paint (Sample.3 D.W.), where (# and *) are Miller indices of peaks attributed to dolomite and calcite, respectively.

Fig. 5 illustrates the XRD data within 10–90° diffraction peak range, with the most relevant peaks corresponding to Dolomite and Calcite. This sample also identified SiO_2 in some amount of amorphous form. These peaks are located at 2θ (Miller indices) = 22.99° (1 0 1), 31.077° (1 0 4), 33.59° (0 0 6), 35.39° (0 1 5), 37.38° (1 1 0), 41.149° (1 1 3), 50.68° (0 1 8), 51.22° (0 1 8), 63.46° (1 2 2) and 67.42° (2 1 4) for dolomite. Calcite peaks are located at 2θ (Miller indices) = 23° (0 1 2), 29.46° (1 0 4), 36.12° (1 1 0), 39.53° (1 1 3), 47.81° (0 1 8) (0 2 4), 48.89° (1 1 6), 57.70° (1 2 2). The results are at per with the research of Debnath & Vaidya, 2006 (Debnath & Vaidya, 2006) and ICSD 073446 (Deng et al., 2010) respectively.

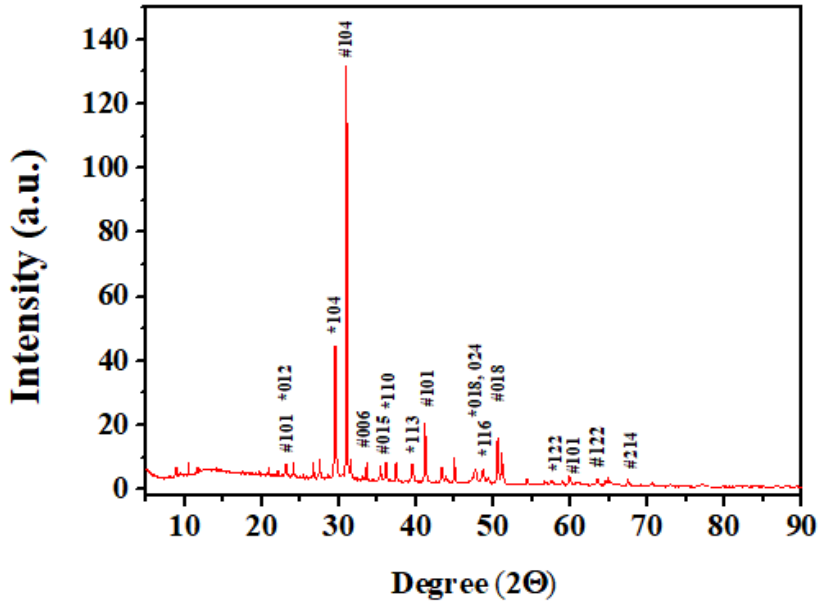

Fig. 6: XRD pattern of used degraded paint flex, where (# and *) are Miller indices of peaks attributed to dolomite and calcite, respectively.

Fig.6 Shows the XRD result in a diffraction angle range of 10–90° consisting of most informative peaks corresponding to dolomite and calcite. These peaks are located at 2θ (Miller indices) = 22.99° (1 0 1), 31.077° (1 0 4), 33.59° (0 0 6), 35.39° (0 1 5), 37.38° (1 1 0), 41.149° (1 1 3), 50.68° (0 1 8), 51.22° (0 1 8), 63.46° (1 2 2) and 67.42° (2 1 4) for dolomite. Calcite peaks are located at 2θ (Miller indices) = 23° (0 1 2), 29.46° (1 0 4), 36.12° (1 1 0), 39.53° (1 1 3), 47.81° (0 1 8) (0 2 4), 48.89° (1 1 6), 57.70° (1 2 2). They are well matched with reference paper Debnath & Vaidya, 2006 (Debnath & Vaidya, 2006) and ICSD 073446 (Deng et al., 2010).

Energy dispersive X-Ray spectroscopy (EDX):

EDX analysis of the same sample is performed to detect and confirm the existence of all components in the sample, as shown in Figs. 7, 8, 9, and 10.

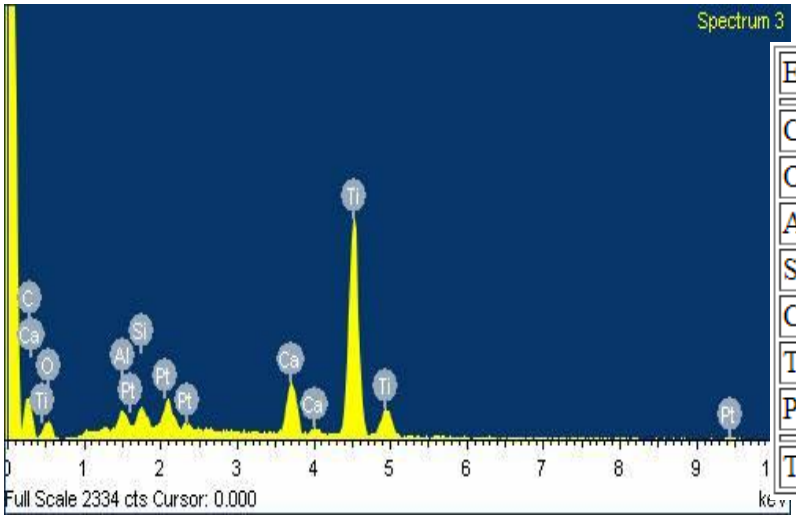

Element	Weight%	Atomic%
C K	24.82	45.69
O K	21.78	30.10
Al K	1.66	1.36
Si K	1.74	1.37
Ca K	5.97	3.29
Ti K	37.88	17.49
Pt M	6.16	0.70
Totals	100.00	

Fig. 7: The representative EDX spectra for water white paint sample.

EDX spectra (Fig.7) indicated the presence of all expected elements clearly and concisely., Ti, C, O, Pt, Ca, Si, Al in the weight percentage of 37.88%, 24.82%, 21.78%, 6.16%, 5.97%, 1.74%, 1.66%, respectively with fewer impurities. It really should be highlighted that the distribution of various components in this sample is critical. The concentration of TiO2 is higher.

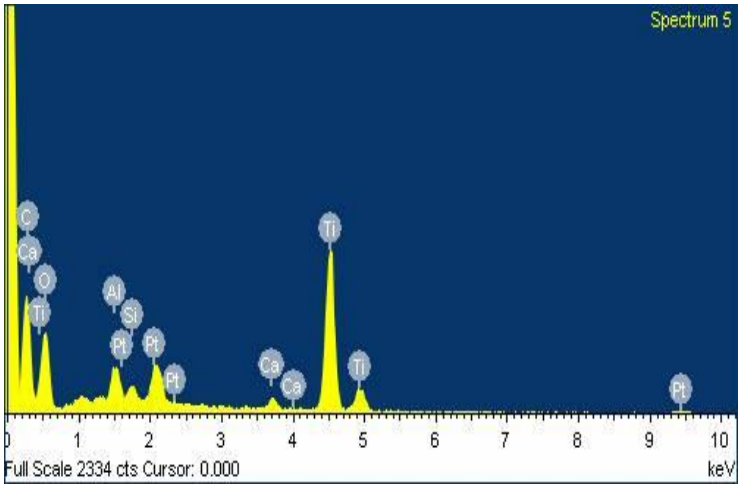

Element	Weight%	Atomic%
C K	36.03	51.22
O K	37.54	40.07
Al K	1.80	1.14
Si K	0.77	0.47
Ca K	0.79	0.34
Ti K	17.67	6.30
Pt M	5.41	0.47
Totals	100.00	

Fig. 8: The representative EDX spectra for solvent paint sample

EDX spectra (Fig. 8) confirm that all of the predicted elements are present, O, C, Ti, Pt, Al, Ca, Si, in the weight percentage of 37.54%, 36.03%, 17.67%, 5.41%, 1.80%, 0.79%, 0.77%, respectively. These spectra confirm the presence of TiO_2 and SiO_2 in the sample.

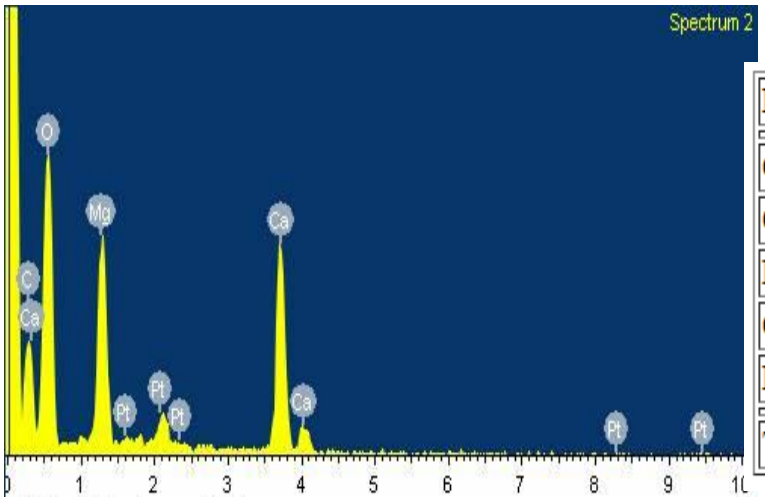

Element	Weight%	Atomic%
C K	25.36	34.57
O K	54.83	56.10
Mg K	7.81	5.26
Ca K	9.44	3.86
Pt M	2.56	0.21
Totals	100.00	

Fig. 9: The representative EDX spectra for distemper white paint sample

The EDX spectra (Fig.9) indicate the presence of all expected elements, O, C, Ca, Mg, Pt, in the weight percentage of 54.83%, 25.36%, 9.44%, 7.81%, 2.56%, respectively. This sample is simply of local paint distemper, so the elemental composition is also different from two fresh paints and no nanoparticles are identified from the sample.

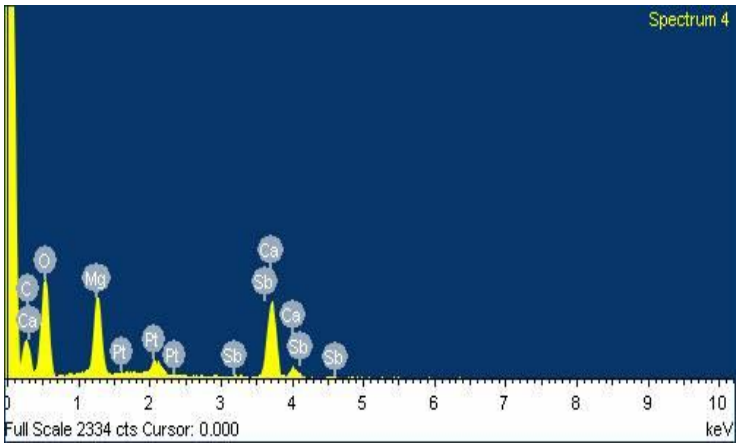

Element	Weight%	Atomic%
C K	22.21	31.79
O K	53.15	57.12
Mg K	8.61	6.09
Ca K	10.12	4.34
Sb L	2.62	0.37
Pt M	3.29	0.29
Totals	100.00	

Fig. 10: The representative EDX spectra for degraded flex paint sample.

The EDX spectra (Fig.10) indicate the presence of all expected elements, O, C, Ca, Mg, Pt, Sb, in the weight percentage of 53.15%, 22.21%, 10.12%, 8.61%, 3.29%, 2.62%, respectively. The degraded sample's elemental composition and weight percentage have not detected any targeted element.

SEM (Scanning Electronic Microscope):

The scanning electron microscopy studies confirmed that the coating surface morphology relies upon composition of the paint. The surface morphology of various paint samples was tested via scanning electron microscopy.

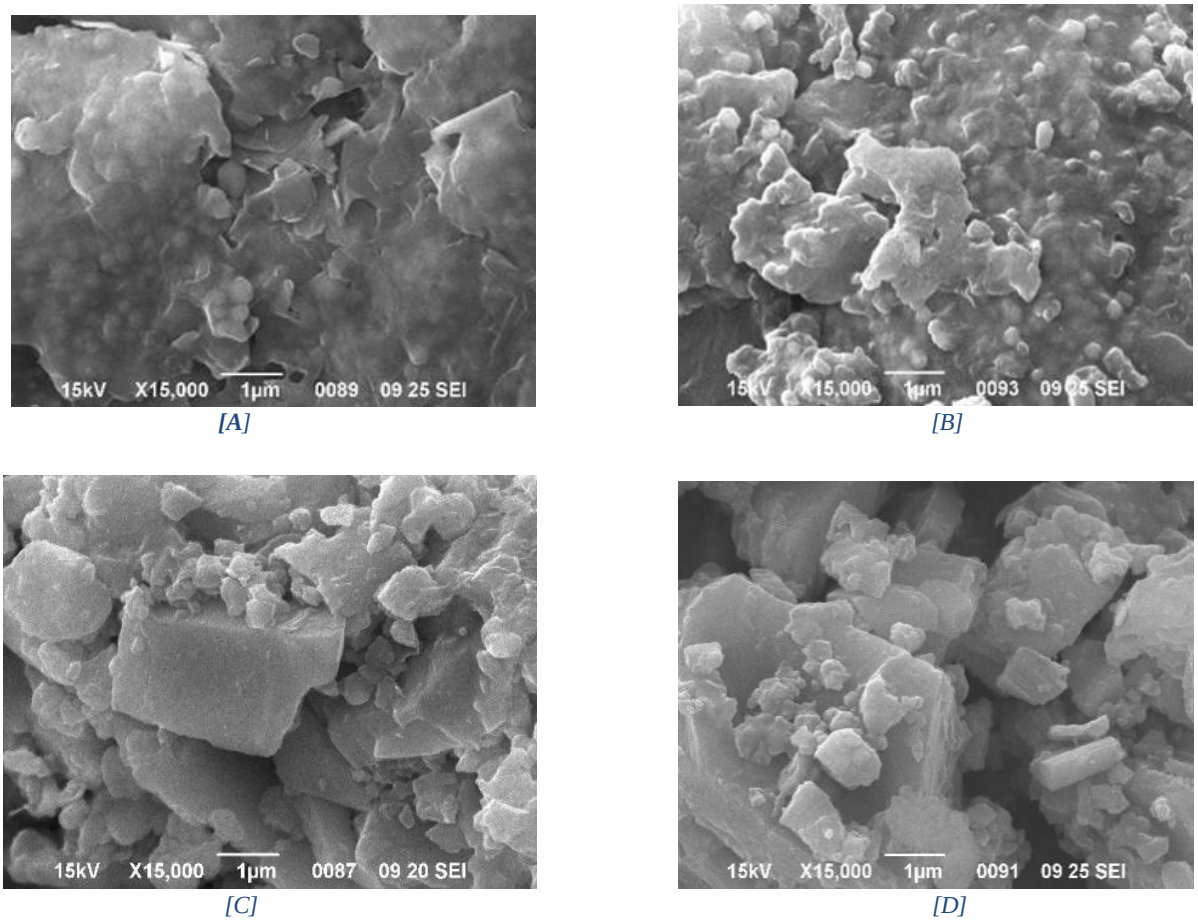

[A] *[B]*

[C] *[D]*

Fig. 11 SEM structural analysis of paint samples

Fig.11 indicates the morphology of paint samples at X15000 magnification. The crosssection of the sample was exposed. The primary one is (A) a water-based paint sample in which more than one graphite layered sheet can be observed. In the thin layer of graphene, the granules shape of TiO_2 can be determined as EDS already confirm the presence of TiO_2.

Fig. 11 (B) represents the spectra of solvent-based white-coloured paint; it can be observed that the sample contains layered granules floor, suggesting the presence of TiO2 and SiO2. Excessive presence of oxygen and carbon were also determined in this sample. Fig. 11 (C) shows that the distemper white paint includes silica debris tightly packed with small spacing and features dice systems. Distemper white is a local paint sample, so the presence of silica is very common while manufacturing. From Fig. 11(D), the small dice shape granules that are tightly packed can be observed.

Discussion:

Characterization of nanoparticles

In the process of characterising nanoparticles, size and shape are two of the most important factors to consider. Along with estimates of the size distribution, degree of aggregation, surface charge, and surface area, the surface chemistry was also evaluated. In addition to particle size, size distribution, and organic ligands on the surface, other characteristics and applications of nanoparticles may be affected. Additionally, the nanoparticles' crystal structure and chemical composition are comprehensively examined as the first step in the characterization process.

Identification of nanoparticles

The XRD analysis confirms the presence of nanoparticles in the first two samples of water-based and solvent-based paints; it shows the crystalline and an amorphous structure, while the other two samples do not contain any nanoparticles. The crystalline structure and morphology of TiO_2 and SiO_2 nanoparticles were studied using XRD. The crystalline character of nanoparticles is indicated by the sharp peak in Fig 3 and Fig 4. X-Ray Diffraction Analysis (or X-Ray Spectroscopy) is a type of X-Ray spectra. In crystallography, x-rays are diffracted by crystalline atoms in a beam of incident X-rays to determine the atomic structure of particles (Rendle, 2019).

Identification of inorganic components

XRD analysis, shown in Figures 5 & 6, identified dolomite CaMg $(CO_3)_2$, Calcite Ca0.936Mg0.064 (CO_3), Magnesium and Barium Niobium Oxide Hydroxide $(Ba_6Nb_3O_{13})$ (O.H.) as the ground layer's components. These results are also supported by Micro XRD analysis in line with the outcomes reported by Lau, who discovered dolomite $CaMg(CO_3)_2$, calcite $(CaCO_3)$, hematite (Fe_2O_3), goethite FeO(O.H.), and lead white 2 Pb $(CO_3)_2$ and Pb $(OH)_2$ as components of the ground layer (Loy et al., 2016; Lau et al., 2006).

Size of particles embedded in paints

Various important pigments and extenders are accessible in both crystalline and amorphous phases. Size distribution, degree of aggregation, surface charge, and surface area can also be measured and to some extent, evaluate the surface chemistry. Size, size distribution and organic ligands present on the surface of the particles may affect other properties and

applications of the nanoparticles. In addition, the crystal structure of the nanoparticles and their chemical composition are thoroughly investigated as the first step of characterization.

Particle size analysis: Particle size analysis was conducted to confirm the particle size for identification of nanoparticles.

The crystallite sizes of the particles are calculated by using **Scherrer's equation.**

$$\boldsymbol{D = \frac{K\lambda}{\beta \cos \theta}}$$

Where

D is the average crystallite size of the particles,

K is a shape factor (K=0.94),

λ is the wavelength of the incident1 X-ray (0.15418 Aº, Cu Kα),

θ is the diffraction angle (Bragg angle) and β is the full width half maximum.

The average particle size of the nanoparticle TiO_2 at its highest peak (27.38^0) is determined by using Debye – Scherer's equation and found to be 60.18 nm. This shows sharp peaks of TiO_2, which indicate the crystallinity of nanoparticles in nature.

Change in quality of paints due to different constituents during manufacturing.

After establishing the standard diffraction pattern of nanoparticles and inorganic compounds in commercial paints, the paint quality differences due to their particles can be thoroughly discussed. Paints are characterised with qualitative differences. Earlier researches indicate that lead (Pb) is used in coatings to speed up the drying process, retain longevity, and improve hydrophobicity; however, TiO_2 nanoparticles are frequently used. Imparting these characteristics enhances the quality of opacity and brightness too. Similarly, SiO_2 has been used in solvent-based paints for strength and bonding; only silica was used instead of SiO_2. Amorphous (non-crystalline) matrix is present in both oil-based and acrylic-based paints (Lau et al., 2006; Fay et al., 2005). The nanoparticle has less impact on health and the environment with higher finishing quality.

Further along with nanoparticles, presence of inorganic substances used in paint was studied and analyzed the XRD pattern of these substances. High amount of Calcite magnesium, dolomite, and barium oxide were identified in whitewash and degraded paints (samples 3 and 4). Inorganic substances have been used for different applications, which are considered necessary when manufacturing paints. To ensure that a paint sample contains standard specifications of the end product, including transparency, pigment, and other mechanical

properties, the most critical is selecting and using the appropriate grade of raw materials for a specific paint's composition.

The nature and composition of extenders used in the formulation of four white paints can easily be distinguished through comparison of emulsion and water-based paints. Besides rutile, which is common in all four formulations, samples S.W. and W.W. contain only TiO_2 nanoparticles while the others contain calcite, clay, and others. Besides these differences, the relative concentrations of rutile and total additives in these samples will likely vary.

Conclusion

X-ray powder diffraction techniques help identify inorganic particles and nanoparticles in many samples. On the other hand, the XRD patterns contain reflected light in oil-based paints due to fillers like calcite, dolomite, and barium niobium oxide hydroxide. The study also concluded that XRD pattern and components percentage are different among all the four samples analyzed due to the physical and chemical differences. XRD data merely is insufficient to determine the whole identity of a paint mixture system. Additional techniques such as EDX can be utilized in association with the XRD process to obtain comprehensive details.

Section-6: Future work

In the biological framework, inhalation of the nanoparticles can easily facilitate the interaction through the living organism via various processes such as its deposition into the blood, adsorption on the surface of the proteins present in the muscles due to its comparable size with proteins present in the muscle. Comparable Nano-size and the sticking properties of the nanoparticles present in the paint have been some of the primary reasons behind these types of interactions through the living organisms; therefore, commercial paint using high-resolution TEM (HR TEM) was analysed in order to confirm nanoparticle's existence in it. By incorporating the HR TEM technique, the size of the particles present in the paint can be easily measured; hence, the Nano scale can be confirmed. Upon confirming the presence of nanoparticles in the commercial paint, their effect on human health can also be examined and demonstrated, accordingly.

Funding: This research is funded by ICSSR Short-term Doctoral Fellowship.

Author's contribution:

First author:

- Analysis and interpretation of data
- I have been involved in drafting the manuscript.
- Agree to be accountable for all aspects of the work in ensuring that questions related to the accuracy or integrity of any part of the work are appropriately investigated and resolved.

The second author (Corresponding author):

- Have made substantial contributions to conception and design
- Revising it critically for important intellectual content
- Have given final approval of the version to be published
- Agree to be accountable for all aspects of the work in ensuring that questions related to the accuracy or integrity of any part of the work are appropriately investigated and resolved

Conflict of Interest:

The authors declare no conflict of interest.

Data availability statements:

No associated data is available.

Acknowledgments:

The study was conducted as an educational and research activity of the Babasaheb Bhimrao Ambedkar University, Lucknow, providing a favourable environment for the study.

References:

Anand, A., Srivastava, V., Singh, S., Shukla, A., Choubey, A. K., & Sharma, A. (2022). Development of nano-enhanced phase change materials using manganese dioxide nanoparticles obtained through green synthesis. *Energy Storage*. https://doi.org/10.1002/est2.344

Chen, M.C, Koh, W.P, Ponnusamy, K.V, Lee, L.S (2022). Titanium dioxide and other nanomaterials based antimicrobial additives in functional paints and coatings: Review, *Progress in Organic Coatings,*163, 106660,

https://doi.org/10.1016/j.porgcoat.2021.106660.

Debnath, N. C., & Vaidya, S. A. (2006). Application of X-ray diffraction technique for characterisation of pigments and control of paints quality. *Progress in Organic Coatings*, *56*(2–3), 159–168. https://doi.org/10.1016/j.porgcoat.2006.03.007

Deng, S., Dong, H., Lv, G., Jiang, H., Yu, B., & Bishop, M. E. (2010). Microbial dolomite precipitation using sulfate reducing and halophilic bacteria: Results from Qinghai Lake, Tibetan Plateau, NW China. *Chemical Geology*, *278*(3–4), 151–159. https://doi.org/10.1016/j.chemgeo.2010.09.008

El-Desoky, M. M., Morad, I., Wasfy, M. H., & Mansour, A. F. (2020). Synthesis, structural and electrical properties of PVA/TiO2 nanocomposite films with different TiO2 phases prepared by sol–gel technique. *Journal of Materials Science: Materials in Electronics*, *31*(20), 17574–17584. https://doi.org/10.1007/s10854-020-04313-7

Fay, F., Linossier, I., Langlois, V., Haras, D., & Vallee-Rehel, K. (2005). SEM and EDX analysis: Two powerful techniques for the study of antifouling paints. *Progress in Organic Coatings*, *54*(3), 216–223. https://doi.org/10.1016/j.porgcoat.2005.05.005

Guglielmi, V., Andreoli, M., Comite, V., Baroni, A., & Fermo, P. (2022). The combined use of SEM-EDX, Raman, ATR-FTIR and visible reflectance techniques for the characterisation of Roman wall painting pigments from Monte d'Oro area (Rome): an insight into red, yellow and pink shades. *Environmental Science and Pollution Research*, *29*(20), 29419–29437. https://doi.org/10.1007/s11356-021-15085-w

Hadimani, R. L. (2018). Rare-Earth Magnetocaloric Thin Films. In *Magnetic Nanostructured Materials: From Lab to Fab*. Elsevier Inc. https://doi.org/10.1016/B978-0-12-813904-2.00009-7

Hiley, C. I., Hansford, G., & Eastaugh, N. (2022). High-resolution non-invasive X-ray diffraction analysis of artists' paints. *Journal of Cultural Heritage*, *53*, 1–13. https://doi.org/10.1016/j.culher.2021.10.008.

Holder, C. F., & Schaak, R. E. (2019). Tutorial on Powder X-ray Diffraction for Characterizing Nanoscale Materials. *ACS Nano*, *13*(7), 7359–7365. https://doi.org/10.1021/acsnano.9b05157

Januzzi & Wolfe (2016). Workplace Injuries. Retived from

https://www.sholljanlaw.com/blog/2016/11/for-professional-painters-the-health-andsafety-risks-cant-be-ignored/ at 13 Oct 2022

Kim, J. H., Hossain, S. M., Kang, H. J., Park, H., Tijing, L., Park, G. W., Suzuki, N., Fujishima, A., Jun, Y. S., Shon, H. K., & Kim, G. J. (2021). Hydrophilic/hydrophobic silane grafting on TiO2 nanoparticles: Photocatalytic paint for atmospheric cleaning. *Catalysts*, *11*(2), 1–21. https://doi.org/10.3390/catal11020193

Lau, D., Hay, D., & Wright, N. (2006). Micro X-ray diffraction for painting and pigment analysis. *AICCM Bulletin*, *30*(1), 38–43. https://doi.org/10.1179/bac.2006.30.1.005

Loganina, V., & Uchaeva, T. (2020). Statistical assessment of damnification risk due to inconformity of paint coating quality. *IOP Conference Series: Materials Science and Engineering*, *962*(2). https://doi.org/10.1088/1757-899X/962/2/022006

Loy, C. W., Matori, K. A., Lim, W. F., Schmid, S., Zainuddin, N., Wahab, Z. A., Alassan, Z. N., & Zaid, M. H. M. (2016). Effects of Calcination on the Crystallography and Nonbiogenic Aragonite Formation of Ark Clam Shell under Ambient Condition. *Advances in Materials Science and Engineering*, *2016*. https://doi.org/10.1155/2016/2914368

Manship, E., Cavallo, G., Gilardi, J., & Riccardi, M. P. (2021). Treating Smalt: A Preliminary SEM-EDX Study of the Effects of Aqueous-based Alkaline Conservation Treatments on Smalt in Wall Paintings. *Studies in Conservation*, *0*(0), 1–16. https://doi.org/10.1080/00393630.2021.1940721

Padmanabhan, Nisha and John, H. (2020). Titanium dioxide based self-cleaning.pdf. *Journal of Environmental Chemical Engineering*, *8*, 104211.

Punmiya, V. (2020). Paint Sector. *Nirmal Bang*, *September*. https://images.assettype.com/bloombergquint/2020-09/162fc669-fb6f-4001-ae74-26c54252da3d/Nirmal_Bang_Paint_Sector_Update_010920.pdf

Rendle, D. F. (2019). International Tables for Crystallography. *Journal of Applied Crystallography*, *7*(2), 738–739. https://doi.org/10.1107/s0021889883010444

Sadiku, E. R., Agboola, O., Agboola, O., Ibrahim, I. D., Olubambi, P. A., Avabaram, B., Bandla, M., Kupolati, W. K., Tippabattini, J., Tippabattini, J., Varaprasad, K., Varaprasad, K., Agwuncha, S. C., Agwuncha, S. C., Mochane, J., Daramola, O. O.,

Oboirien, B., Adegbola, T. A., Nkuna, Chima, B. (2018). Nanotechnology in Paints and Coatings. In *Advanced Coating Materials* (Issue December). https://doi.org/10.1002/9781119407652.ch7

Solano, R., Patiño-Ruiz, D., & Herrera, A. (2020). Preparation of modified paints with nano-structured additives and its potential applications. *Nanomaterials and Nanotechnology*, *10*, 1–17. https://doi.org/10.1177/1847980420909188

Srinivas, K. (2018). Nanotechnology in Paint Industry. *International Journal of TechnoChem Research*, *04*(01), 27–39.

Thakur, P., Kumar, R., Kumar, S., Pathania, A., & Goel, B. (2021). Analysis and optimization of properties of paint materials for reduction of paint defects in agro products. Materials Today: Proceedings, 45, doi:10.1016/j.matpr.2021.02.349